Current Research in Food Science 8 (2024) 100778

Contents lists available at ScienceDirect

Current Research in Food Science

journal homepage: www.sciencedirect.com/journal/current-research-in-food-science

Non-covalent complexes of lutein/zeaxanthin and whey protein isolate formed at different pH levels: Binding interactions, storage stabilities, and bioaccessibilities

Gang Zhang [a], Xin Qi [a], Linlin He [a], Xiao Wang [a,c], Yanna Zhao [a], Qingpeng Wang [a], Jun Han [a,c], Zhengping Wang [a,b], Zhuang Ding [a,b,*], Min Liu [a]

[a] Institute of Biopharmaceutical Research, Liaocheng University, Liaocheng, 252059, China
[b] Shandong Liang-Jian Biotechnology Co., Ltd., Zibo, 255000, China
[c] Liaocheng High-Tech Biotechnology Co., Ltd., Liaocheng, 252059, China

ARTICLE INFO

Handling Editor: Xing Chen

Keywords:
Xanthophylls
Whey protein isolate
Complexation
Functional properties
pH changes

ABSTRACT

Lutein (Lut) and zeaxanthin (Zx) are promising healthy food ingredients; however, the low solubilities, stabilities, and bioavailabilities limit their applications in the food and beverage industries. A protein-based complex represents an efficient protective carrier for hydrophobic ligands, and its ligand-binding properties are influenced by the formulation conditions, particularly the pH level. This study explored the effects of various pH values (2.5–9.5) on the characteristics of whey protein isolate (WPI)–Lut/Zx complexes using multiple spectroscopic techniques, including ultraviolet–visible (UV–Vis), fluorescence, and Fourier transform infrared (FTIR) spectroscopies and dynamic light scattering (DLS). UV–Vis and DLS spectra revealed that Lut/Zx were present as H-aggregates in aqueous solutions, whereas WPI occurred as nanoparticles. The produced WPI–Lut/Zx complexes exhibited binding constants of 10^4–10^5 M^{-1}, which gradually increased with increasing pH from 2.5 to 9.5. FTIR spectra demonstrated that pH variations and Lut/Zx addition caused detectable changes in the secondary WPI structure. Moreover, the WPI–Lut/Zx complexes effectively improved the physicochemical stabilities and antioxidant activities of Lut/Zx aggregates during long-term storage and achieved bioaccessibilities above 70% in a simulated gastrointestinal digestion process. The comprehensive data obtained in this study offer a basis for formulating strategies that can be potentially used in developing commercially available WPI complex-based xanthophyll-rich foods.

1. Introduction

Lutein (β,ε-carotene-3,3'-diol, Lut) and zeaxanthin (β,β-carotene-3,3'-diol, Zx) are critical xanthophyll carotenoids that are characterized by the presence of multiple conjugated double bonds in polyenic chains and dipolar terminally hydroxylated β- or ε-ionone rings in their structures. They are also known as macular pigments because of their ability to cross the blood–retina barrier and accumulate in the macular region of the retina. Several studies have shown that a supplementary intake of Lut and Zx effectively protects the eyes from high-energy light- and oxidative stress-induced retinal damage, further reducing the risk of macular degeneration (Mares-Perlman et al., 2001). Other benefits of Lut and Zx include maintaining human cognitive health and preventing cardiovascular diseases and several types of cancer (Kim and Shin, 2022; Xu et al., 2022), which render Lut and Zx promising natural nutrients. However, as extremely hydrophobic compounds, Lut and Zx are not easily released from the food matrix into the digestive lumen, which limits their bioaccessibilities (Steiner et al., 2018; Zhang et al., 2024). Furthermore, as food supplements, Lut and Zx are sensitive to oxygen, acid, light, and heat; thus, they are easily degraded during food production, storage, and digestion. Therefore, the oral bioavailabilities of Lut and Zx are considerably limited by their hydrophobic and unstable chemical structures (Becerra et al., 2020).

Protein-based encapsulation and complexation are promising methods for enhancing the solubilities and stabilities of carotenoids (Cheng et al., 2023). Whey protein isolate (WPI) is a critical source of nutritious functional peptides, which is widely utilized in the food processing industry because of its excellent solubilization,

* Corresponding author.
E-mail address: dingzhuang@lcu.edu.cn (Z. Ding).

https://doi.org/10.1016/j.crfs.2024.100778
Received 5 February 2024; Received in revised form 5 May 2024; Accepted 26 May 2024
Available online 28 May 2024

emulsification, and film formability properties and broad application range (Akbarbaglu et al., 2021). WPI comprises multiple globular proteins, predominantly including β-lactoglobulin (~60%) and α-lactalbumin (~22%) (Allahdad et al., 2019). Their surfaces contain abundant binding sites, enabling non-covalent interactions with various small-molecule ligands, such as anthocyanins, flavonoids, polyphenols, and vitamins (Akbarbaglu et al., 2021). WPI has also been widely investigated for its potential use in protecting and delivering carotenoid compounds, including Lut, β-carotene, fucoxanthin, lycopene, bixin, and norbixin (Mantovani et al., 2021). These studies revealed the existence of strong interactions between WPI and carotenoids, which are primarily driven by hydrophobic forces. Yi et al. (2016) studied WPI–Lut complexes in an aqueous environment at pH = 7.4 and found that the chemical stability of Lut was significantly improved over a storage period of 16 d due to its binding to WPI.

pH is a critical parameter in preparing food and beverage products that significantly affects the conformations and charge characteristics of food proteins, further influencing complexation with other bioactive molecules (Allahdad et al., 2019; Lelis et al., 2023). The influence of pH changes on the binding affinity of small molecules to proteins varies significantly owing to the differences in binding sites between various ligand molecules. Liang and Subirade (2012) found that decreasing pH from 7.4 to 2.0 reduced the binding strengths of folic acid and tocopherol to β-lactoglobulin, while the binding strength of resveratrol remained unaffected. Allahdad et al. (2019) investigated the interactions between WPI and β-carotene across the pH range of 4–9. They observed a significant increase in their binding affinity only at pH = 9 compared with the other pH conditions. Zhu et al. (2020) reported that the affinity between β-lactoglobulin and apigenin decreased in the order of pH 6.2 > 8.2 > 7.1 > 2.6. Liu et al. (2022) found that the interaction strength between β-lactoglobulin and epigallocatechin-3-gallate increased gradually as the pH increased from 2.5 to 7.0. Additionally, pH is one of the most important factors affecting the chemical stability of nutritional compounds. For instance, Lut and Zx are chemically more stable under neutral and alkaline conditions than under acidic conditions (Becerra et al., 2020). Meanwhile, pH variations may influence the binding mechanisms by inducing alterations in the chemical states of small molecules. For instance, norbixin dissolves under neutral and alkaline conditions and forms stable aggregates under acidic conditions (Møller et al., 2020), which may affect its binding to WPI.

As critical food ingredients, the physicochemical properties of macromolecular WPI and small-molecule Lut/Zx are affected by changes in pH, which may influence the interactions and stabilities of WPI–Lut/Zx complexes; however, related studies have not been conducted yet. In this work, WPI–Lut/Zx complexes were prepared in the pH range 2.5–9.5 and their performance characteristics and interactions were examined using multiple spectroscopic techniques, including ultraviolet–visible (UV–Vis), fluorescence spectroscopy, and dynamic light scattering (DLS). The stabilities of Lut and Zx in the WPI–Lut/Zx complexes under different pH conditions and their bioaccessibilities were evaluated. The surface hydrophobicities and secondary structures of these complexes helped achieve a better understanding of the changes in the chemical stabilities and bioaccessibilities of the two xanthophylls.

2. Materials and methods

2.1. Materials

Lut (CAS# 127-40-2; UV purity: 90%) and Zx (CAS# 144-68-3; UV purity: 90%) were purchased from Shandong Tianyin Biotechnology (Zibo, China), and Lut (LOT#00012453-3B1) and Zx (LOT#00026504-3E) standards used in quantitative analysis were acquired from ChromaDex (Los Angeles, CA, USA). WPI (EuriNutri 90) was purchased from Eurial Ingredients and Nutrition (Nantes, France), and deionized water was obtained using a Milli-Q Advantage A10 water purification system (MilliporeSigma, Burlington, MA, USA). Chromatography-grade acetonitrile and methanol were purchased from Thermo Fisher Scientific (Waltham, MA, USA), and dimethyl sulfoxide (DMSO), 6-propionyl-2-(*N,N*-dimethylamino) naphthalene (PRODAN), and other reagents were purchased from Sinopharm Chemical Reagent (Shanghai, China). A total antioxidant capacity assay kit (T-AOC; LOT#R24146) was obtained from Shanghai Yuanye Bio-Technology (Shanghai, China).

2.2. Sample preparation

WPI was dissolved in phosphate-buffered saline (PBS, 10 mM, pH = 7.5) at 25 °C and gently stirred overnight at 4 °C for complete hydration. The obtained WPI solution was adjusted to a required pH value (2.5, 5.5, 7.5, or 9.5) using aqueous hydrochloric acid (1 M) or sodium hydroxide (1 M) and diluted with PBS to yield a 50 μM WPI stock solution. The apparent relative molecular mass of WPI was 20 kDa (Meng et al., 2021). Crude Lut and Zx powders were dissolved in DMSO to yield 100–450 μM stock solutions. To prepare WPI–Lut/Zx complexes, a Lut or Zx stock solution (5 vol%) was slowly added to the WPI solution under slow stirring, and the Lut/Zx concentrations in the final systems ranged from 5 to 22.5 μM. The WPI working concentrations utilized in spectroscopic analysis and stability studies were 5 and 22.5 μM, respectively. DMSO was used as a dispersing adjuvant for Lut/Zx, and its concentration was maintained at 5 vol% to avoid substantial changes in the WPI state, as determined by the protein size distribution (Fig. S1).

2.3. Spectral analysis

2.3.1. UV–Vis spectroscopy

UV–Vis spectroscopy was conducted using a UV-2401PC spectrometer (Shimadzu, Kyoto, Japan).

2.3.2. DLS

The particle size distributions of the WPI working solutions (22.5 μM) with and without DMSO (5 vol%) were measured via DLS using a Zetasizer Nano ZSP system (Malvern Panalytical, Malvern, UK).

2.3.3. Fluorescence spectroscopy

Fluorescence spectroscopy was performed using an F-7000 fluorescence spectrophotometer (Hitachi, Tokyo, Japan) equipped with a temperature controller. The WPI–Lut/Zx complexes were prepared under different pH conditions according to the method described in Section 2.2, yielding protein-to-xanthophyll molar ratios of 1:0, 1:1, 1:1.5, 1:2, 1:2.5, 1:3, 1:3.5, 1:4, and 1:4.5. The samples were excited at 280 nm after incubation for 30 min at 25 °C, and fluorescence spectra were recorded in the range 300–500 nm. The slit widths used during excitation and emission were set to 5 nm, and the scan rate was 1200 nm min^{-1}. The influences of the solvent and inner filter effects of the studied complexes were eliminated according to the procedure developed by Yi et al. (2016).

2.3.4. Fourier transform infrared spectroscopy

Fourier transform infrared (FTIR) spectra (4000–500 cm^{-1}) of WPI with and without Lut/Zx were recorded using a Nicolet iS10 FTIR spectrometer (Thermo Fisher Scientific). Solutions of WPI–Lut/Zx complexes were prepared with the concentration of each component equal to 22.5 μM. The complex solutions were incubated for 30 min at 25 °C and lyophilized to yield dry powders (2.0 mg) that were ground with potassium bromide powder (100 mg) and pressed into flakes for FTIR studies. The protein secondary structure content was calculated based on the secondary derivative in the 1600–1700 cm^{-1} amide I region using PeakFit 4.12 software (Inpixon, Palo Alto, CA, USA) (Cui et al., 2021).

2.4. Surface hydrophobicity determination

The surface hydrophobicity values (H_0) of WPI with and without

Lut/Zx were determined at different pH values using the uncharged fluorescent probe PRODAN (Haskard and Li-Chan, 1998). The WPI solutions (0–22.5 μM) and corresponding complexes containing Lut/Zx (5 μM) were prepared at pH = 2.5, 5.5, 7.5, and 9.5. After incubation at 25 °C for 30 min, each sample (4 mL) was mixed with 10 μL of the PRODAN solution (1.5 mM, DMSO) and then incubated for 15 min at 25 °C. The fluorescence intensity of each solution was measured using the F-7000 spectrophotometer with the excitation/emission slits and wavelengths set to 5/5 nm and 365/465 nm, respectively. The fluorescence intensity of the corresponding sample without PRODAN was measured simultaneously and subtracted to yield the corrected fluorescence. H_0 was calculated using the slope of the linear regression of the fluorescence intensity as a function of the WPI concentration.

2.5. Storage stability

2.5.1. Sample preparation

The storage stabilities of the WPI–Lut/Zx complexes over 30 d were determined at different pH values using an MKF 720 climatic chamber (Binder, Tuttlingen, Germany). The concentration of each component of the WPI–Lut/Zx complexes was maintained at 22.5 μM, and sodium azide (0.01 wt%) was added to prevent bacterial growth. Samples containing only Lut or Zx were prepared as blank groups to enable a physical stability comparison. The dispersant Tween 80 (0.01%, w/w) was added to the blank samples as a control to enable a chemical stability comparison. This concentration of Tween 80 was used because its aggregated form was comparable to those of the WPI–Lut/Zx complexes (Fig. S2). The samples were placed in sealed glass vials and stored for 30 d at 40 °C.

2.5.2. Physical stability

The average particle sizes of the WPI–Lut/Zx complexes before and after 30 d of storage were determined using the Zetasizer Nano ZSP system (Malvern Panalytical) to assess their physical stabilities.

2.5.3. Appearance and color measurements

The appearances of the WPI–Lut/Zx complexes were recorded before and after 30 d of storage using a digital camera with a 28-mm lens (Zfc, Nikon, Tokyo, Japan) under white light irradiation with an illuminance of approximately 100 lx. Their color characteristics (L^*, a^*, and b^*) were measured using a CS-821N colorimeter (CHN Spec, Hangzhou, China) in the reflectance mode. The total color difference (ΔE) was calculated using the CIELAB color difference formula: $\Delta E = [(L^* - L_0^*)^2 + (a^* - a_0^*)^2 + (b^* - b_0^*)^2]^{1/2}$ (Zahoor et al., 2023). L^* (lightness), a^* (red–green chromaticity), and b^* (blue–yellow chromaticity) denote the CIELAB colorimetric values of the samples after 30 d of storage, and L_0^*, a_0^*, and b_0^* are their initial colorimetric values.

2.5.4. Chemical stability

During the 30-d storage period, sample aliquots (1 mL) were withdrawn at predetermined time intervals. An organic solvent (hexane: acetone = 2:1, v/v, total volume: 6 mL) was added to the filtered aqueous sample (1 mL) to extract Lut/Zx species. After centrifugation at 2000×*g* for 2 min (25 °C), the organic phase was carefully collected and dried under a stream of nitrogen gas. The extracted samples were redissolved in methanol and analyzed using a Dionex UltiMate 3000 high-performance liquid chromatograph (Thermo Fisher Scientific) and C18 analytical column (QuikSep SP ODS-A, 5 μm, 4.6 × 250 mm, H&E, Beijing, China). The content of Lut/Zx was determined in the range 1–50 μM using a standard curve method. The retention rate (RR) was calculated using the following equation: $\%RR = C_{time}/C_{sample}$. Here, C_{time} denotes the residual amount (μM) at a specific sampling time during 30 d of storage, and C_{sample} is the initial amount of Lut/Zx (22.5 μM).

The degradation kinetics of Lut/Zx were analyzed using the linear decay equation: $Y_R = 100 - k\,X$, where Y_R, X, k, and 100 denote the retention rate (%) of Lut/Zx, storage time (d), degradation coefficient (%/d), and initial rate of 100%, respectively.

2.6. Antioxidant activity

The antioxidant activities of the WPI–Lut/Zx complexes before and after 30 d of storage were measured using T-AOC and the 2,2'-azino-bis (3-ethylbenzothiazoline-6-sulfonic acid)$^+$ (ABTS)$^+$ method according to manufacturer's instructions. The ABTS radical stock solution was prepared by mixing 7 mM ABTS–$(NH_4)_2$ and 2.45 mM potassium persulfate solutions (1:1, v/v) for 16 h at 25 °C in the dark. An ABTS radical working solution was obtained by diluting the stock solution with ethanol until its absorbance reached 0.700 ± 0.020 at 734 nm. One hundred microliters of the complex sample or distilled water (blank) were mixed with 100 μL of the ABTS working solution and incubated at 25 °C for 15 min in the dark. The absorbance of the prepared mixture was measured at 734 nm using a BioTek ELX800 microplate reader (Agilent Technologies, Santa Clara, CA, USA), and the scavenging activity (%) was calculated using the following equation: ABTS scavenging rate (%) = $(A_{blank} - A_{sample})/A_{blank} \times 100$.

2.7. Bioaccessibility

In vitro simulated gastrointestinal digestion was performed to evaluate the effects of the WPI–Lut/Zx complexes on the bioavailabilities of Lut and Zx. The simulation procedure was conducted using an SHA-CA thermostatic water–bath oscillator (Putian Instruments, Changzhou, China) according to the INFOGEST 2.0 protocol (Brodkorb et al., 2019) with slight modifications (Iddir et al., 2020). A simulated gastric fluid (SGF) was prepared as follows: a mixture of pepsin (6.4 mg mL^{-1}) and calcium chloride (0.15 mM) was adjusted to pH = 3.0. A simulated intestinal fluid (SIF) was a mixture of trypsin (2 mg mL^{-1}), bile salts (6.8 mg mL^{-1}), and calcium chloride (0.6 mM) adjusted to pH = 7.0. The simulated digestion fluids were prewarmed at 37 °C prior to in vitro digestion. Gastric digestion was simulated by mixing the samples and SGF (1:1, v/v), adjusting the pH to 7.0, and then incubating for 2 h at 37 ± 0.5 °C with stirring at 100 rpm. After gastric digestion, the gastric chyme was mixed with an equivalent volume of SIF, the pH was adjusted to 7.0, and incubation was continued at 37 ± 0.5 °C for 2 h. The obtained digest (12 mL) was immediately transferred to ice at the end of the intestinal digestion process.

The digested samples were centrifuged at 3200×*g* for 1 h (4 °C) to separate the micellar phase of the supernatant, and the intermediate aqueous phase (2 mL) was collected and filtered through a 0.2-μm membrane. The micellized Lut or Zx in the aqueous phase was further extracted and analyzed as described in Section 2.5.4, and the bioaccessibilities of the xanthophylls were calculated by dividing the amount of the micellized Lut or Zx by the amount initially added to the digestion model (Iddir et al., 2020).

2.8. Statistical analysis

All experiments were conducted in triplicate, and the results are reported as means ± standard deviations. Numerical data were compared using *t*-tests in GraphPad Prism 9.5 (GraphPad Software, Boston, MA, USA), and the statistical significance was set to $P < 0.05$.

3. Results and discussion

3.1. Oligomeric states of protein particles and small molecules

3.1.1. H-aggregation states of Lut/Zx

In previous studies on protein–carotenoid complexes, simplified models have frequently been adopted to elucidate the mechanisms of molecular interactions between the monomers of proteins and carotenoids (Rasera et al., 2023). The structural aspects of proteins and

carotenoids and their influences on complex interactions may be easily ignored (Mantovani et al., 2021; Lelis et al., 2023). The Lut/Zx form was first examined via UV–Vis absorption spectroscopy. As typically hydrophobic compounds, carotenoids form only monodisperse states in certain organic solvents, where carotenoid monomers exhibit visible absorption in the range 425–525 nm corresponding to the $S_0 \rightarrow S_2$ electronic transitions of the conjugated polyene structures. Nevertheless, the absorption intensities of carotenoids in the polar aqueous phase decrease significantly coupled with blue or red shifts, representing the spectral characteristics of carotenoid H-type and J-type aggregates, respectively (Zhu et al., 2019). Fig. S3 shows that Lut/Zx species in the complexes exhibit the maximum absorption wavelengths of 383 and 390 nm. These species represent typical H-type aggregates, which are characterized by the "card-packed" structures comprising several carotenoid monomers (Fig. S4) (Hempel et al., 2016; Rasera et al., 2023). In addition, the UV absorption spectra indicate that the Lut/Zx absorption intensities increase linearly with increasing Lut/Zx concentration (5–22.5 μM, $R > 0.99$) while no significant spectral shifts are observed. Therefore, the aggregation states of Lut and Zx in these samples remain consistent.

3.1.2. WPI nanoaggregates

The nanoaggregate state of WPI was examined by measuring the hydrodynamic diameter of 5 μM WPI in the aqueous solution via DLS. Except for pH = 5.5, the particle size distributions of WPI at the other pH levels exhibit similar dominant peaks at approximately 200 nm (Fig. S1). However, owing to the attenuation of charge repulsion around the isoelectric point (pI), WPI particles undergo further self-assembly at pH = 5.5 and form larger particles with sizes of 400 nm (Fig. S1). According to the study of Allahdad et al. (2019), the diameter of WPI is 5.2 nm due to the contributions from the main fractions, such as α-lactalbumin (3.4 nm), β-lactoglobulin (3.7 nm), and bovine serum albumin (5.5 nm). Hence, the single dominant peak in the DLS profile obtained in this study indicates that WPI produces nanoaggregates at a concentration of 5 μM in aqueous media. Moreover, the size distribution is not significantly altered by the incorporation of DMSO (5%, v/v).

3.2. Binding interactions studied via fluorescence spectroscopy

3.2.1. Interactions between Lut/Zx and WPI

Fluorescence spectroscopy was used to characterize the interactions between WPI and both xanthophylls. The fluorescence emission spectra of WPI recorded at different concentrations of the two xanthophylls and xanthophyll/protein molar ratios ranging from 0 to 4.5 are shown in Fig. 1. During excitation at 280 nm, WPI exhibits a strong fluorescence emission peak at 334 nm, which is attributed to its tryptophan (Trp) residues (Yi et al., 2016). The incorporation of Lut/Zx leads to the fluorescence quenching of WPI, and the fluorescence intensity decreases progressively with increasing Lut/Zx concentration (Fig. 1). Fluorescence quenching may be caused by various processes, including excited-state reactions, energy transfer, complex formation, and collision quenching (Allahdad et al., 2018). To elucidate the mechanism of WPI quenching by Lut/Zx, the classic Stern–Volmer model was used to fit the fluorescence data according to the following equation: $F_0/F = 1 + K_{SV}[Q] = 1 + Kq\,\tau_0[Q]$, where F and F_0 are the fluorescence intensities of WPI with and without Lut/Zx, respectively; K_{SV} and Kq represent the dynamic Stern–Volmer and quenching rate constants, respectively; τ_0 is the fluorescence lifetime of the protein, which is equal to approximately 10^{-8} s; and [Q] is the Lut/Zx concentration. The fitting results reveal that the Stern–Volmer curves of the fluorescence quenching of WPI by Lut/Zx obtained at each pH value (2.5–7.5) are linear ($R^2 > 0.99$). The calculated Kq values (3.62×10^{12}–7.91×10^{12} L mol^{-1} s^{-1}) are two orders of magnitude higher than the limiting diffusion quenching constant (2.0×10^{10} L mol^{-1} s^{-1}) for biological macromolecules, indicating that the mechanism of WPI quenching by Lut/Zx is static (Ren et al., 2022).

For static quenching, the binding constant (K_b) and number of binding sites (n) were determined using the linear relationship $\log(F_0/F - 1)$ as a function of $\log[Q]$: $\log(F_0/F - 1) = \log K_b + n\log[Q]$ (Fig. S5 and Table 1). In this study, the K_b values of Lut and Zx binding to WPI at

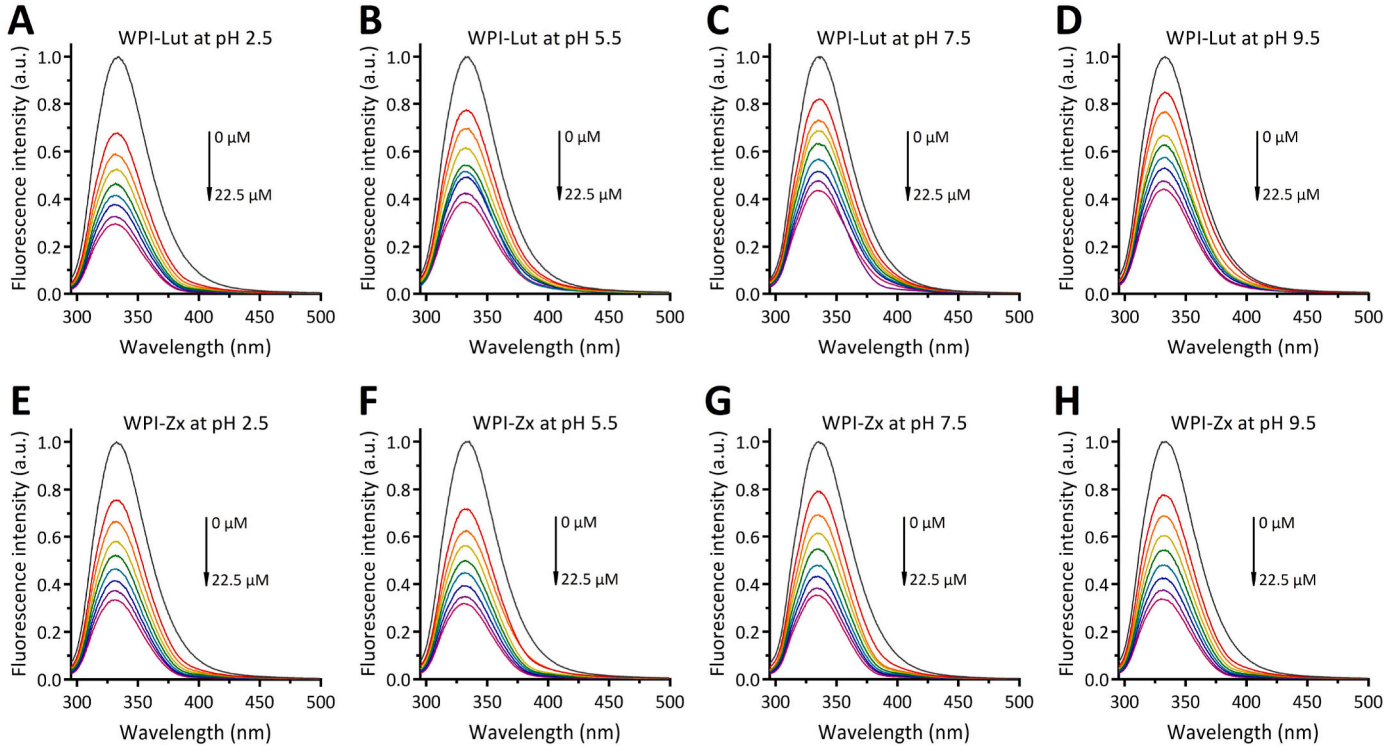

Fig. 1. Normalized fluorescence spectra of 5 μM whey protein isolate (WPI) with various concentrations of lutein (Lut) or zeaxanthin (Zx) at different pH levels (**A**–**D**: Lut-WPI at pH 2.5–9.5; **E**–**H**: Zx-WPI at pH 2.5–9.5).

Table 1
Quenching (K_q) and binding constants (K_b) of the interactions between whey protein isolate (WPI) and lutein/zeaxanthin (Lut/Zx) and the number of binding sites (n) under different pH conditions.

Complex	pH	K_q ($\times 10^{12}$ M^{-1} s^{-1})	K_b ($\times 10^4$ M^{-1})	N
WPI-Lut	2.5	7.91 ± 0.20	2.17 ± 0.15	0.88 ± 0.03
	5.5	4.76 ± 0.13	1.19 ± 0.15	0.87 ± 0.03
	7.5	3.62 ± 0.09	2.21 ± 0.19	0.96 ± 0.04
	9.5	3.77 ± 0.10	3.87 ± 0.14	1.00 ± 0.03
WPI-Zx	2.5	5.76 ± 0.07	3.77 ± 0.07	0.96 ± 0.01
	5.5	6.34 ± 0.16	2.29 ± 0.18	0.91 ± 0.04
	7.5	4.93 ± 0.11	12.36 ± 0.10	1.09 ± 0.02
	9.5	5.63 ± 0.17	15.45 ± 0.13	1.10 ± 0.03

different pH levels are 1.19×10^4–3.87×10^4 and 2.29×10^4–15.45×10^4 M^{-1}, respectively. Therefore, these WPI-xanthophyll complexes exhibit strong non-covalent binding interactions, and the complexes of Zx with WPI exhibit higher affinities than those of Lut with WPI under the same conditions. The K_b values of the WPI-xanthophylls obtained in this study are lower than those reported by Yi et al. (2016) who investigated the interactions of WPI with Lut at pH = 7.4 and obtained K_b values of 2.4×10^5–3.5×10^5 M^{-1} because of the higher concentration of protein (~25 μM), which attenuated the aggregation of Lut and promoted its binding to proteins. Hence, Allahdad et al. (2019) obtained a lower K_b value (0.52×10^4 M^{-1}) at pH = 7.0 in a study on the interactions between β-carotene and WPI, which was conducted at a lower WPI concentration of 1 μM.

3.2.2. *Effect of pH on molecular interactions*

The effects of pH on the K_b values of WPI and Lut/Zx are illustrated in Table 1. When the pH value is reduced from alkaline (9.5) to acidic (2.5), K_b gradually decreases (Table 1), indicating that Lut/Zx binds more strongly to WPI in alkaline aqueous environments. Specific pH conditions influence the protein structure and charge characteristics, which affect the binding of WPI and Lut/Zx. Our findings are generally consistent with those of several previous studies, which reported stronger binding between milk proteins and hydrophobic compounds, such as β-lactoglobulin and bikinin (Zhang et al., 2013) and WPI and β-carotene (Allahdad et al., 2019), at higher pH values. These results suggest that protein molecules are more loosely structured at higher pH levels, exposing more hydrophobic regions and thus facilitating the attachment of hydrophobic compounds. Previous studies on the β-lactoglobulin structure conducted at different pH values revealed that at higher pH values, the E–F loop in the β-lactoglobulin structure rearranged to expose the hydrophobic calyx, resulting in a protein conformational exchange from the closed to open conformations (Uhrínová et al., 2000). Remarkably, the lowest K_b values were obtained for WPI and Lut/Zx at pH = 5.5 because protein molecules underwent self-aggregation via hydrophobic interactions when the pH of the environment was close to the pI of WPI, thus decreasing the number of exposed hydrophobic cavities that might capture small molecules.

3.3. *Secondary structure of WPI determined by FTIR*

FTIR spectroscopy is a commonly used technique for studying the secondary structures of proteins and their conformational changes. To investigate the effects of pH and xanthophyll addition on the protein secondary structure, WPI and WPI–Lut/Zx complexes were analyzed in terms of the amide I regions (1600–1700 cm^{-1}) of their FTIR spectra recorded at different pH values (2.5, 5.5, 7.5, and 9.5; see Fig. S6). The calculated contents of α-helices, β-sheets, β-turns, and random coils are listed in Table 2. As the pH increases from 2.5 to 9.5, the β-sheet contents of WPI and WPI–Lut/Zx complexes gradually decrease, whereas their random coil contents increase. Similar phenomena were observed by Wang et al. (2023), who reported that a higher pH level decreased the β-sheet contents and increased the random coil contents of lysogel/gelatin proteins. These trends reveal a higher degree of structural unfolding of proteins at the higher pH levels (He et al., 2021). Unlike WPI, most WPI–Lut/Zx complexes do not exhibit significant changes in their content distributions of the protein secondary structures because Lut/Zx binds to the hydrophobic protein surface as H-aggregates. Nevertheless, the incorporation of Zx at the higher pH levels of 7.5 and 9.5 slightly decreases the β-sheet content of WPI. The fluorescence analysis results confirmed that the WPI–Zx complexes exhibited the high binding constants of 10^5 M^{-1} at the higher pH levels of 7.5 and 9.5. The higher affinities between WPI and Zx benefit from the more open conformation of WPI at the larger pH values. Thus, the stronger binding between Zx and WPI at the high pH levels may slightly change the WPI conformation. Zhao et al. (2022) investigated the interactions between Lut and red bean proteins. The β-sheet contents of the resulting red bean protein–Lut complexes decreased to 29.5% as compared with that of the pure protein of 31.9%. Similar effects were observed for β-lactoglobulin upon binding to several polyphenolic compounds (Qie et al., 2020; Meng and Li, 2021).

Table 2
Secondary structures of whey protein isolate (WPI) in the absence and presence of lutein/zeaxanthin (Lut/Zx) under different pH conditions.

Sample	pH	α-helix (%)	β-sheet (%)	Turn (%)	Random coil (%)
WPI	2.5	18.5 ± 0.6	31.1 ± 0.1	31.7 ± 0.2	18.7 ± 0.7
	5.5	18.6 ± 0.3	28.9 ± 0.4	34.7 ± 0.8	17.8 ± 1.1
	7.5	19.4 ± 0.4	24.9 ± 0.2	35.2 ± 0.5	20.5 ± 0.5
	9.5	22.3 ± 0.4	19.7 ± 0.3	37.5 ± 0.8	20.4 ± 0.9
WPI-Lut	2.5	18.6 ± 0.3	31.2 ± 0.6	32.1 ± 0.2	18.1 ± 0.9
	5.5	18.2 ± 0.4	28.7 ± 0.6	34.7 ± 0.2	18.4 ± 0.7
	7.5	20.2 ± 0.3	24.7 ± 0.8	35.1 ± 0.4	20.0 ± 0.3
	9.5	22.4 ± 0.9	19.1 ± 0.7	38.4 ± 0.6	20.1 ± 0.7
WPI-Zx	2.5	18.7 ± 0.5	31.3 ± 0.4	31.9 ± 0.1	18.1 ± 0.3
	5.5	19.5 ± 0.3	28.3 ± 0.4	33.6 ± 0.6	18.6 ± 0.1
	7.5	19.8 ± 0.3	22.5 ± 0.7	38.6 ± 0.1	19.1 ± 0.6
	9.5	23.1 ± 0.9	18.6 ± 0.2	38.0 ± 0.4	20.3 ± 0.5

3.4. *Surface hydrophobicity of complexes*

The surface hydrophobicity values (H_0) of WPI and the WPI–Lut/Zx complexes formed in this study are shown in Fig. 2. A gradual increase in H_0 is observed with increasing pH from acidic to neutral to basic. This trend is consistent with that reported by Alizadeh-Pasdar and Li-Chan (2000), who measured the H_0 values of WPI and bovine serum albumin using the same fluorescence method based on PRODAN. At the higher pH levels, the structures of WPI molecules become looser, and more surface hydrophobic groups are exposed, while binding between carotenoids and natural proteins is mainly mediated by hydrophobic interactions. Thus, the observed increase in H_0 with increasing pH is consistent with the K_b values; however, the H_0 values of all samples at pH = 9.5 decrease slightly as compared with those at pH = 7.5. This may be due to the enhancement of protein self-assembly caused by the larger exposed hydrophobic regions at a higher WPI concentration of 25 μM used in the H_0 study.

As shown in Fig. 2, the H_0 of WPI is significantly reduced after binding to Lut/Zx ($P < 0.05$). Hydrophobic compounds form hydrophobic interactions with specific amino acid residues of the protein polypeptide chain (e.g., tryptophan residues). As the higher fraction of surface hydrophobic residues is covered with Lut/Zx, the number of PRODAN bound to WPI decreases, resulting in a lower H_0 value (Cui et al., 2021). In addition, the interaction of Lut/Zx with WPI changes the structural conformation of the protein, exposing several hidden hydrophilic regions, which may be another cause of the reduced H_0 value of WPI (Kroll et al., 2000; Rawel et al., 2002).

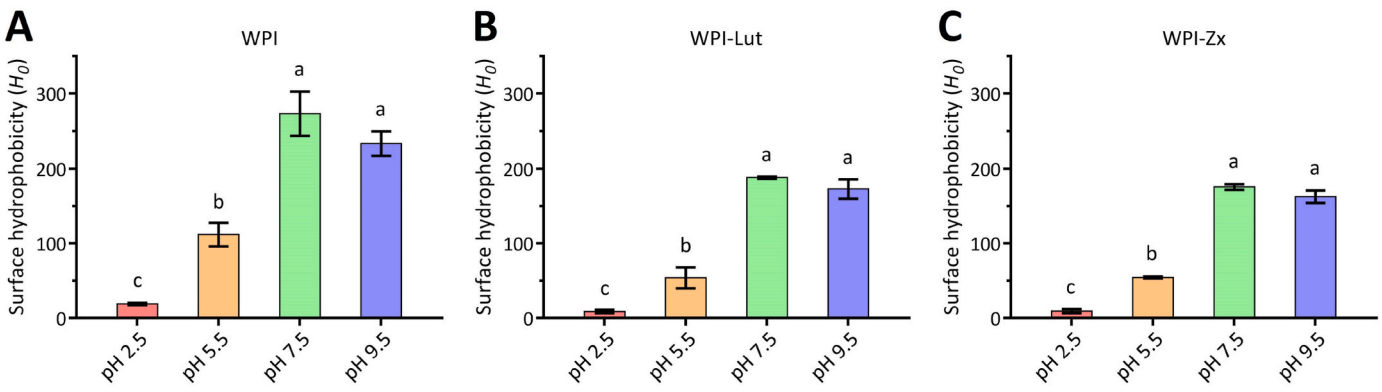

Fig. 2. Surface hydrophobicities (H_0) of whey protein isolate (WPI) under different pH conditions [**A**: pure protein; **B**: WPI-lutein (Lut) complexes; **C**: WPI-zeaxanthin (Zx) complexes].

3.5. Storage stability

3.5.1. Physical and color stability

To investigate the effect of WPI complexation on the physical stability of Lut/Zx, changes in the particle sizes of the WPI–Lut/Zx complexes and blank and control groups were examined over 30 d of storage (Table 3). The results obtained for the blank group (formulations without stabilizers) are not shown because of the severe agglomeration of Lut/Zx particles with micrometer-scale sizes (0 d: 2.89–9.28 μm; 30 d: 3.26–19.13 μm). In the control group (formulations with Tween 80), the Lut/Zx particle sizes increase from the initial 98.3–114.6 nm to 203.5–266.4 nm after 30 d. Hence, the application of the low-concentration surfactant can help generate suitable Lut/Zx particle sizes during preparation but insufficient for maintaining their physical stabilities during long-term storage. In addition, the results obtained for the control groups reveal that the Lut/Zx particle sizes are unaffected by the pH levels of 2.5–9.5. The particle sizes of the WPI–Lut/Zx complexes at each pH level remain constant after 30 d of storage. In particular, the particle sizes of the complexes at pH = 5.5 are maintained at a high value of 400 nm because of protein particle aggregation, and those obtained at the other pH values are approximately 200 nm. Therefore, the addition of WPI increases the physical stability of Lut/Zx.

The color of a liquid food is one of the most important characteristics influencing consumer's choice, and the initial appearances of the evaluated samples under different pH conditions are shown in Fig. S7. The fresh formulations containing Zx display darker yellow colors than those of the formulations containing Lut. The difference in pH produces no detectable effects on the visual appearances of similar formulations. Compared with the control group, the complexes are slightly paler in color, which may be related to the light-shading effects of protein particles. The blank samples without stabilizers display the lightest colors because of the aggregation of xanthophyll particles. The colors of these samples observed after 30 d of storage at 40 °C are shown in Fig. 3. After the accelerated stability study, the samples exhibit different degrees of discoloration. Compared with the control group, the color losses of the complexes are significantly reduced because of their relatively high Lut/Zx contents owing to the protective effect of WPI. The color changes of the samples before and after the stability study were quantified by calculating their ΔE values (Fig. S8) (Zahoor et al., 2023). The ΔE values of all the evaluated formulations increase gradually as the pH decreases from 9.5 to 2.5. The control group exhibits the most distinct color change with the ΔE values of 16.8–19.9 for Lut and 18.8–23.2 for Zx. The ΔE values of the complexes decrease to 8.6–14.8 for Lut and 8.3–17.5 for Zx. Similarly, the blank group displays clear color losses due to xanthophyll degradation, which is consistent with the results of the chemical stability assay of Lut/Zx.

Table 3
Particle size (PS) stabilities of the different formulations containing lutein (Lut) and zeaxanthin (Zx) under different pH conditions over 30 d of storage at 40 °C.

Sample	pH	PSs of Lut-loaded samples (nm)		PSs of Zx-loaded samples (nm)	
		initial	After 30 d	initial	After 30 d
Control	2.5	112.2 ± 22.1	235.8 ± 38.6	104.7 ± 9.2	266.4 ± 23.9
	5.5	105.8 ± 13.4	216.5 ± 23.3	114.6 ± 12.3	249.0 ± 37.6
	7.5	113.6 ± 14.2	228.6 ± 44.2	104.6 ± 36.0	238.8 ± 19.9
	9.5	98.3 ± 17.3	203.5 ± 33.2	102.4 ± 7.5	214.6 ± 16.6
WPI	2.5	196.0 ± 7.3	212.1 ± 15.1	189.2 ± 7.2	203.0 ± 23.7
	5.5	371.2 ± 21.9	373.5 ± 25.8	318.1 ± 33.5	318.6 ± 46.1
	7.5	199.8 ± 12.7	192.1 ± 14.2	197.7 ± 23.3	198.5 ± 20.4
	9.5	198.4 ± 23.6	207.2 ± 18.3	194.9 ± 32.0	196.3 ± 17.0

3.5.2. Chemical stability

Fig. 4 shows the degradation kinetics of Lut and Zx in the different formulations observed at pH levels of 2.5–9.5 over 30 d of storage. The degradation curves of both xanthophylls over 30 d conform to the linear decay model (R^2 = 0.8648–0.9988). The degradation coefficients k of Lut and Zx calculated for all samples are listed in Table 4. In the control groups, the k values of Lut and Zx determined at pH values ranging from 9.5 to 2.5 are equal to 1.51–2.75 and 1.58–2.34 %/d, respectively. Based on the results obtained for the control groups, Lut and Zx in their H-aggregated states exhibit enhanced chemical stabilities at alkaline pH values as compared with those observed under acidic conditions, and the chemical stability of Zx under acidic conditions is significantly higher than that of Lut. The additional 5',7'-conjugated double bond in the Zx structure endows it with higher chemical stability as compared with Lut, which contains a 4'-allylic hydroxyl group (Bernstein et al., 2016). Compared with the control groups, the addition of WPI significantly reduces the degradation rate of Lut/Zx with Lut and Zx exhibiting k values of 1.13–1.90 and 1.03–1.55 %/d obtained in the pH range from 9.5 to 2.5, respectively. Furthermore, the protective effects of the WPI complexes on the chemical stability of Lut/Zx are more distinct at pH = 7.5 with the highest Δk values of 0.90 and 0.87 obtained for Lut and Zx, respectively. This result is associated with the higher binding affinities of xanthophylls to WPI at elevated pH values (Table 1). In addition, the blank groups without stabilizers exhibit lower k values (1.15–1.45 %/d for Lut and 0.99–1.30 %/d for Zx), which may be due to the barrier protective effects caused by the excessive self-aggregation of Lut and Zx.

3.6. $ABTS^+$ radical scavenging activity

The antioxidant activities of the WPI–Lut/Zx complexes under different pH conditions and those of the blank and control samples were evaluated after 30 d of storage using the $ABTS^+$ assay (Fig. 5). The $ABTS^+$ radical scavenging activities of the studied samples positively correlate with the xanthophyll concentration. The $ABTS^+$ free radical scavenging rates of the control groups in the pH range from 2.5 to 9.5 are

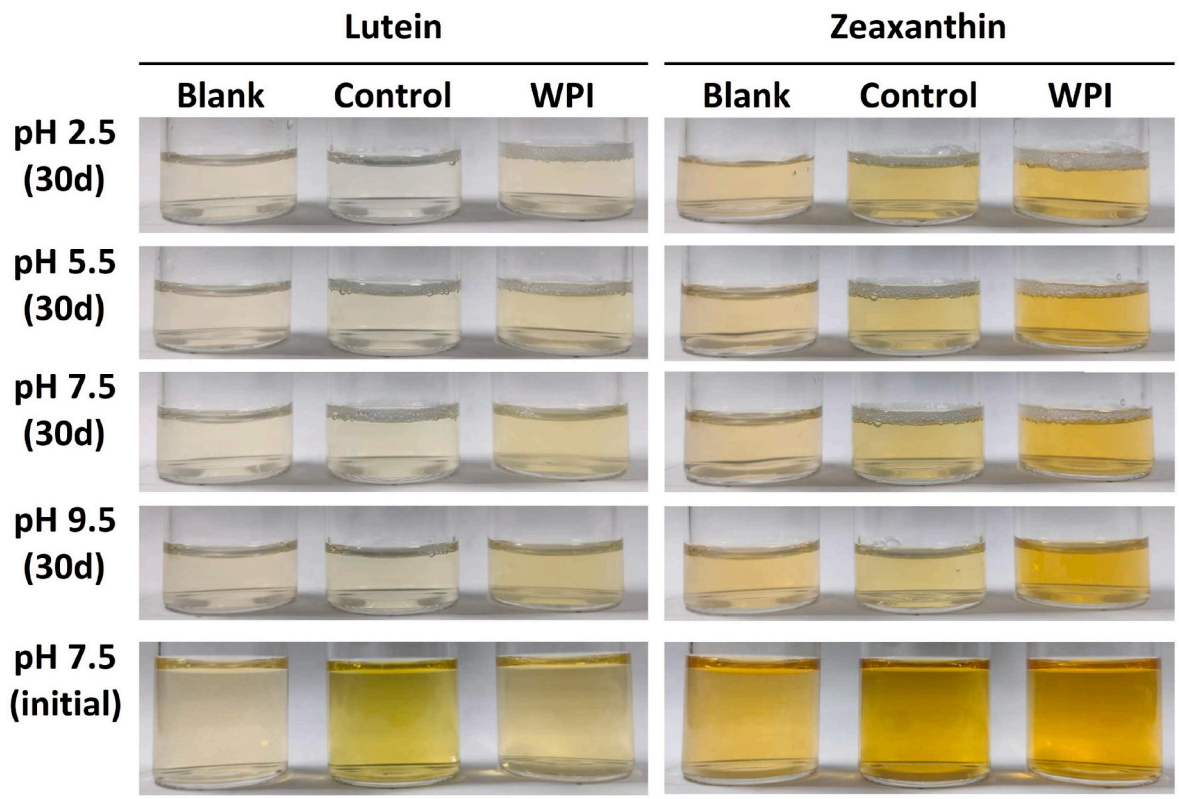

Fig. 3. Appearance development of the different formulations containing lutein/zeaxanthin (Lut/Zx, 22.5 μM) under different pH conditions (Blank formulations do not contain protein or stabilizers; control formulations contain 0.01 wt% Tween 80; WPI indicates the WPI-Lut/Zx complexes).

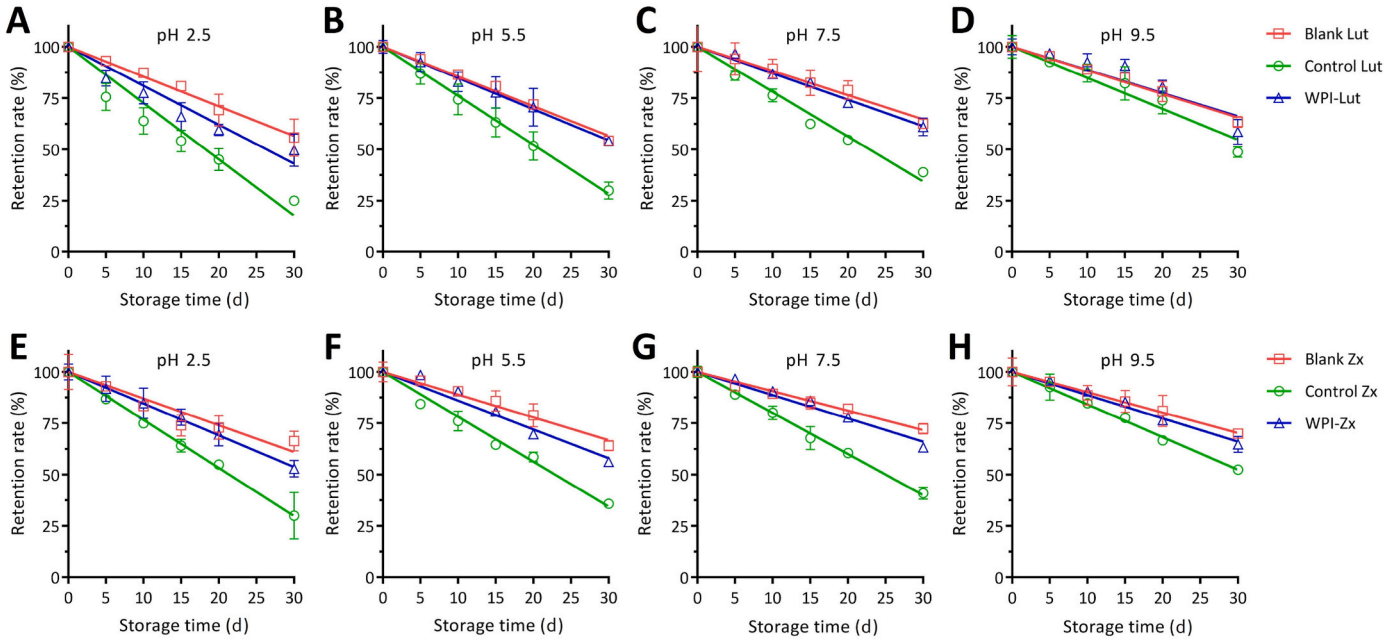

Fig. 4. Chemical stabilities of lutein/zeaxanthin (Lut/Zx, 22.5 μM) in the absence and presence of whey protein isolate (WPI, 22.5 μM) under different pH conditions over 30 d of storage at 40 °C (**A**–**D**: formulations containing Lut at pH 2.5–9.5; **E**–**H**: formulations containing Zx at pH 2.5–9.5; blank formulations do not contain protein or a stabilizer; control formulations contain 0.01 wt% Tween 80).

only 11.0–14.4% for Lut and 26.6–33.9% for Zx. Meanwhile, the free radical scavenging rates of the complexes increase to 43.4–83.4% for Lut and 53.0–87.1% for Zx, respectively, indicating that WPI binding effectively preserves the chemical stability of Lut/Zx and thus maintains their antioxidative properties. In addition, the formation of WPI complexes increases the xanthophyll dispersity in liquid systems, which promotes the release of Lut/Zx and their ability to exert antioxidative effects. In contrast, the blank samples display lower free radical scavenging capacities (16.0–25.1% for Lut and 41.1–47.1% for Zx) despite their high Lut/Zx retention rates, which are attributed to the excessive

Table 4
Degradation coefficients *k* of lutein (Lut) and zeaxanthin (Zx) in the different formulations over 30 d of storage at 40 °C.

Sample	Lut (%/d)				Zx (%/d)			
	pH 2.5	pH 5.5	pH 7.5	pH 9.5	pH 2.5	pH 5.5	pH 7.5	pH 9.5
Blank	1.45	1.45	1.18	1.15	1.30	1.11	0.95	0.99
Control	2.75	2.39	2.19	1.51	2.34	2.18	2.00	1.58
Complex	1.90	1.52	1.29	1.13	1.55	1.40	1.13	1.03
Δk [a]	0.85	0.87	0.9	0.38	0.79	0.78	0.87	0.55

[a] Δk is the difference between the degradation coefficients of the control and complex samples, and it represents the improvement in the chemical stability of Lut/Zx via complexation with WPI.

aggregation of Lut/Zx species. The large aggregates in the blank samples prevented the release of Lut/Zx molecules, inhibiting their antioxidant activities.

3.7. Bioaccessibility

Xanthophylls entering the gastrointestinal tract should undergo release, emulsification, and micellization for the uptake by enterocytes (Kopec and Failla, 2018), and the proportion of micellized xanthophylls represents the amount of xanthophylls that may be absorbed or bioaccessible in the gut (Desmarchelier and Borel, 2017; Mantovani et al., 2022). Generally, the bioavailabilities of carotenoids depend on their bioaccessibilities (Nwachukwu et al., 2016; Becerra et al., 2020); therefore, improving the bioaccessibilities and thus bioavailabilities of xanthophylls is a critical objective in developing oral xanthophyll products. Fig. 6 shows the bioaccessibilities of Lut and Zx in the WPI–Lut/Zx complexes as well as those in the blank and control groups determined after in vitro digestion. Differences in the initial pH levels do not influence xanthophyll bioaccessibility in the same formulation because after mixing with the SGF, all the studied samples have a uniform pH environment. The bioaccessibilities of Lut (73.3–77.2%) and Zx (78.4–80.3%) combined with WPI improve significantly relative to those of the blank samples (38.2–41.5% for Lut and 42.0–47.7% for Zx), and these values are comparable to those of the control groups (69.9–77.2% for Lut and 74.5–77.4% for Zx). Proteins are amphiphilic molecules with surface activities and emulsifying properties, which enhance the dispersion and release of liposoluble components in aqueous media and promote emulsification and micellization during gastrointestinal digestion (McClements and Li., 2010; Cheng et al., 2023). Zhao et al. (2022) reported the beneficial effects of red bean protein–Lut complexes on the bioaccessibility of Lut, which resulted in a 71.0% release during simulated gastrointestinal digestion. However, high protein concentrations may decrease the bioaccessibilities of lipophilic components, particularly when these components are incorporated into lipid droplets via emulsion (Qiu et al., 2015). Iddir et al. (2020) reported that the presence of 3–7.5 mg mL^{-1} WPI decreased the bioaccessibility of lutein in an emulsion system. In this case, excess protein molecules are adsorbed on the oily droplet surface and form a barrier resistant to digestion, hindering the release of the lipophilic constituents. In this study, the bioaccessibilities of the xanthophylls are significantly enhanced at a WPI–Lut complex concentration of 22.5 μM (~0.45 mg mL^{-1}).

4. Conclusion

This study investigated the interactions between Lut/Zx and WPI influenced by the pH of the aqueous medium and the effects of these interactions on the antioxidant activities, storage stabilities, and bioaccessibilities of the two xanthophylls. The obtained UV and DLS spectra indicated that the xanthophylls and WPI existed in the forms of H-aggregates and nanoparticles, respectively, in their aqueous solutions. The fluorescence spectroscopy data revealed that the quenching of WPI by

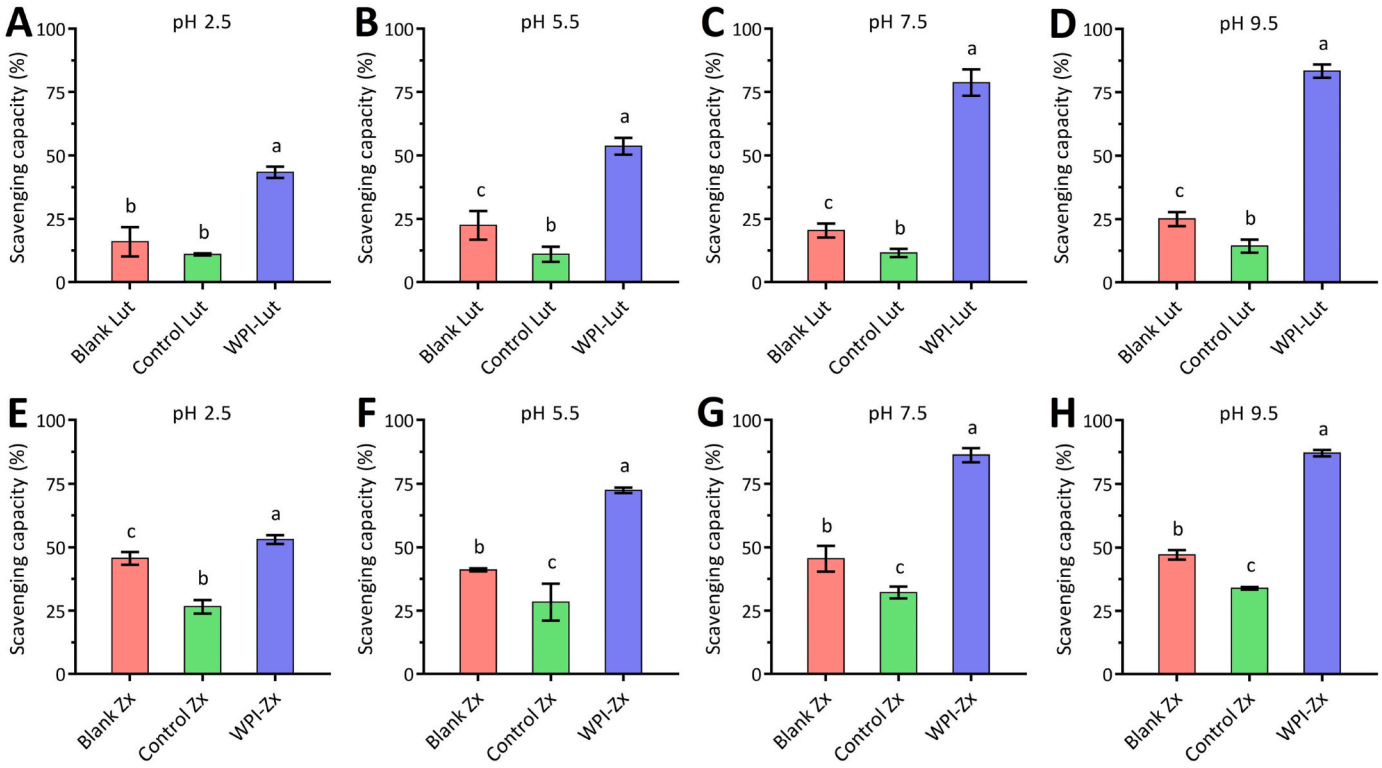

Fig. 5. ABTS $^{+}$ scavenging activities of the different formulations containing lutein/zeaxanthin (Lut/Zx, 22.5 μM) under different pH conditions after 30 d of storage at 40 °C (**A**–**D**: Formulations containing Lut at pH 2.5–9.5; **E**–**H**: Formulations containing Zx at pH 2.5–9.5; blank formulations do not contain protein or stabilizers; control formulations contain 0.01 wt% Tween 80).

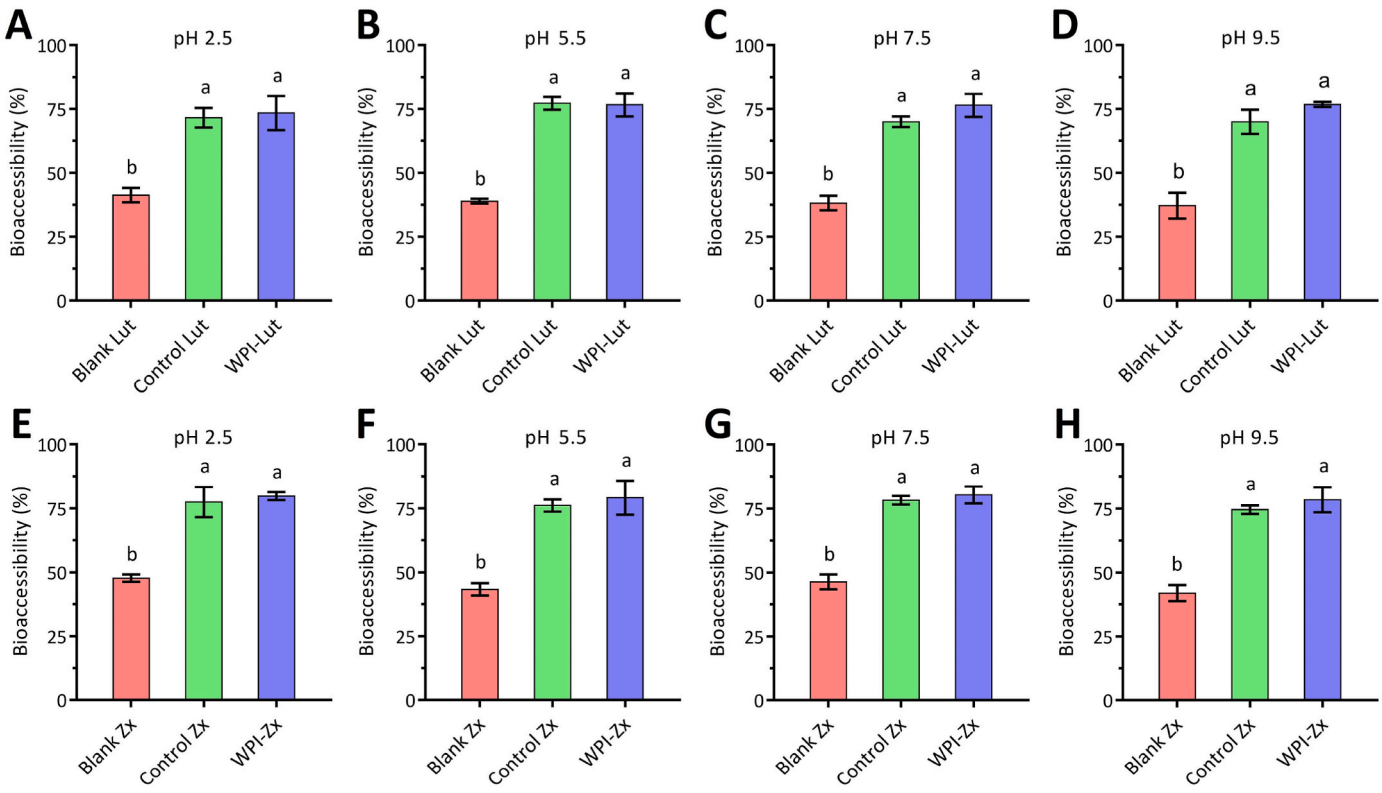

Fig. 6. Bioaccessibilities of lutein (Lut) and zeaxanthin (Zx) in the different formulations prepared under different pH conditions (**A**–**D**: Formulations containing Lut at pH 2.5–9.5; **E**–**H**: Formulations containing Zx at pH 2.5–9.5; blank formulations without protein or stabilizers; control formulations containing 0.01 wt% Tween 80).

Lut/Zx was mainly static and that their binding affinities generally increased with increasing pH from 2.5 to 9.5. The FTIR spectroscopy analysis of the protein secondary structures demonstrated that increasing the pH level caused the unfolding of the WPI structure, resulting in the exposure of more hydrophobic regions, which was consistent with the results of the H_0 assay. The performance evaluation of WPI–Lut/Zx indicated that the presence of WPI significantly protected the xanthophylls against aggregation and degradation, thus improving their bioactivity and accessibility. Our study provides a theoretical basis and experimental data for the development of an effective WPI-based xanthophyll delivery system, which can be applied in the industrial production of healthy beverage products.

CRediT authorship contribution statement

Gang Zhang: Methodology, Formal analysis, Writing – original draft. **Xin Qi:** Methodology, Formal analysis. **Linlin He:** Methodology, Formal analysis. **Xiao Wang:** Methodology. **Yanna Zhao:** Data curation. **Qingpeng Wang:** Project administration, Funding acquisition. **Jun Han:** Supervision. **Zhengping Wang:** Funding acquisition, Writing – review & editing. **Zhuang Ding:** Conceptualization, Funding acquisition, Writing – review & editing. **Min Liu:** Methodology, Funding acquisition, Writing – review & editing.

Declaration of competing interest

The authors declare that they have no competing financial interests or personal relationships that may have influenced the work reported in this study.

Data availability

Data will be made available on request.

Acknowledgements

This work was supported by the National Natural Science Foundation of China (No. 22073039), Natural Science Foundation of Shandong Province (No. ZR2021MD123), and Youth Innovation Technology Project of Higher School in Shandong Province (No. 2021KJ099). This work was technically supported by Zhejiang Nutrasis Biotech (Taizhou, China) and the Taishan Scholar Research Group.

Appendix A. Supplementary data

Supplementary data to this article can be found online at https://doi.org/10.1016/j.crfs.2024.100778.

References

Akbarbaglu, Z., Peighambardoust, S.H., Sarabandi, K., Jafari, S.M., 2021. Spray drying encapsulation of bioactive compounds within protein-based carriers; different options and applications. Food Chem. 359, 129965 https://doi.org/10.1016/j.foodchem.2021.129965.

Alizadeh-Pasdar, N., Li-Chan, E.C.Y., 2000. Comparison of protein surface hydrophobicity measured at various pH values using three different fluorescent probes. J. Agric. Food Chem. 48 (2), 328–334. https://doi.org/10.1021/jf990393p.

Allahdad, Z., Varidi, M., Zadmard, R., Saboury, A.A., 2018. Spectroscopic and docking studies on the interaction between caseins and β-carotene. Food Chem. 255, 187–196. https://doi.org/10.1016/j.foodchem.2018.01.143.

Allahdad, Z., Varidi, M., Zadmard, R., Saboury, A.A., Haertlé, T., 2019. Binding of β-carotene to whey proteins: multi-spectroscopic techniques and docking studies. Food Chem. 277, 96–106. https://doi.org/10.1016/j.foodchem.2018.10.057.

Becerra, M.O., Contreras, L.M., Lo, M.H., Díaz, J.M., Herrera, G.C., 2020. Lutein as a functional food ingredient: stability and bioavailability. J. Funct.Foods 66, 103771. https://doi.org/10.1016/j.jff.2019.103771.

Bernstein, P.S., Li, B., Vachali, P.P., Gorusupudi, A., Shyam, R., Henriksen, B.S., Nolan, J. M., 2016. Lutein, zeaxanthin, and meso-zeaxanthin: the basic and clinical science underlying carotenoid-based nutritional interventions against ocular disease. Prog. Retin. Eye Res. 50, 34–66. https://doi.org/10.1016/j.preteyeres.2015.10.003.

Brodkorb, A., Egger, L., Alminger, M., Alvito, P., Assunção, R., Ballance, S., Bohn, T., Bourlieu-Lacanal, C., Boutrou, R., Carrière, F., Clemente, A., Corredig, M.,

Dupont, D., Dufour, C., Edwards, C., Golding, M., Karakaya, S., Kirkhus, B., Feunteun, S.L., Lesmes, U., Macierzanka, A., Mackie, A.R., Martins, C., Marze, S., McClements, D.J., Ménard, O., Minekus, M., Portmann, R., Santos, C.N., Souchon, I., Paul Singh, R., Vegarud, G.E., Wickham, M.S.J., Weitschies, W., Recio, I., 2019. INFOGEST static in vitro simulation of gastrointestinal food digestion. Nat. Protoc. 14 (4), 991–1014. https://doi.org/10.1038/s41596-018-0119-1.

Cheng, H., Chen, W., Jiang, J., Khan, M.A.Wusigale, Liang, L., 2023. A comprehensive review of protein-based carriers with simple structures for the co-encapsulation of bioactive agents. Compr. Rev. Food Sci. Food Saf. 22 (3), 2017–2042. https://doi.org/10.1111/1541-4337.13139.

Cui, Q., Dong, Y., Zhang, A., Wang, X., Zhao, X., 2021. Multiple spectra analysis and calculation of the interaction between Anthocyanins and whey protein isolate. Food Biosci. 44, 101353 https://doi.org/10.1016/j.fbio.2021.101353.

Desmarchelier, C., Borel, P., 2017. Overview of carotenoid bioavailability determinants: from dietary factors to host genetic variations. Trends Food Sci. Technol. 69, 270–280. https://doi.org/10.1016/j.tifs.2017.03.002.

Haskard, C.A., Li-Chan, E.C.Y., 1998. Hydrophobicity of bovine serum albumin and ovalbumin determined using uncharged (PRODAN) and anionic (ANS-) fluorescent probes. J. Agric. Food Chem. 46 (7), 2671–2677. https://doi.org/10.1021/jf970876y.

He, W., Yin, Z., Liu, S., Chen, Y., Qie, X., Chen, J., Zeng, M., Qin, F., He, Z., 2021. Effect of preheated milk proteins and bioactive compounds on the stability of cyanidin-3-O-glucoside. Food Chem. 345, 128829 https://doi.org/10.1016/j.foodchem.2020.128829.

Hempel, J., Schädle, C.N., Leptihn, S., Carle, R., Schweiggert, R.M., 2016. Structure related aggregation behavior of carotenoids and carotenoid esters. J. Photochem. Photobiol., A 317, 161–174. https://doi.org/10.1016/j.jphotochem.2015.10.024.

Iddir, M., Dingeo, G., Porras Yaruro, J.F., Hammaz, F., Borel, P., Schleeh, T., Desmarchelier, C., Yvan Larondelle, Y., Bohn, T., 2020. Influence of soy and whey protein, gelatin and sodium caseinate on carotenoid bioaccessibility. Food Funct. 11 (6), 5446–5459. https://doi.org/10.1039/D0FO00888E.

Kim, M.J., Shin, W.S., 2022. Stability of zeaxanthin/lutein in yolk oil obtained from microalgae-supplemented egg under various storage conditions. LWT–Food Sci. Technol. 155, 112899 https://doi.org/10.1016/j.lwt.2021.112899.

Kopec, R.E., Failla, M.L., 2018. Recent advances in the bioaccessibility and bioavailability of carotenoids and effects of other dietary lipophiles. J. Food Compos. Anal. 68, 16–30. https://doi.org/10.1016/j.jfca.2017.06.008.

Kroll, J., Rawel, H.M., Seidelmann, N., 2000. Physicochemical properties and susceptibility to proteolytic digestion of myoglobin-phenol derivatives. J. Agric. Food Chem. 48 (5), 1580–1587. https://doi.org/10.1021/jf991172m.

Lelis, C.A., Galvan, D., Conte-Junior, C.A., 2023. Nanocarriers for β-carotene based on milk protein. Food Bioprocess Technol. 16 (1), 43–67. https://doi.org/10.1007/s11947-022-02868-3.

Liang, L., Subirade, M., 2012. Study of the acid and thermal stability of b-lactoglobulin-ligand complexes using fluorescence quenching. Food Chem. 132, 2023–2029. https://doi.org/10.1016/j.foodchem.2011.12.043.

Liu, C., Lv, N., Xu, Y.Q., Tong, H., Sun, Y., Huang, M., Ren, G., Shen, Q., Wu, R., Wang, B., Cao, Z., Xie, H., 2022. pH-dependent interaction mechanisms between β-lactoglobulin and EGCG: insights from multi-spectroscopy and molecular dynamics simulation methods. Food Hydrocolloids 133, 108022. https://doi.org/10.1016/j.foodhyd.2022.108022.

Mantovani, R.A., Rasera, M.L., Vidotto, D.C., Mercadante, A.Z., Tavares, G.M., 2021. Binding of carotenoids to milk proteins: why and how. Trends Food Sci. Technol. 110, 280–290. https://doi.org/10.1016/j.tifs.2021.01.088.

Mantovani, R.A., Xavier, A.A.O., Tavares, G.M., Mercadante, A.Z., 2022. Lutein bioaccessibility in casein-stabilized emulsions is influenced by the free to acylated carotenoid ratio, but not by the casein aggregation state. Food Res. Int. 161, 111778 https://doi.org/10.1016/j.foodres.2022.111778.

Mares-Perlman, J.A., Fisher, A.I., Klein, R., Palta, M., Block, G., Millen, A.E., Wright, J. D., 2001. Lutein and zeaxanthin in the diet and serum and their relation to age-related maculopathy in the third national health and nutrition examination survey. Am. J. Epidemiol. 153 (5), 424–432. https://doi.org/10.1093/aje/153.5.424.

McClements, D.J., Li, Y., 2010. Structured emulsion-based delivery systems: controlling the digestion and release of lipophilic food components. Adv. Colloid Interface Sci. 159, 213–228. https://doi.org/10.1016/j.cis.2010.06.010.

Meng, Y., Li, C., 2021. Conformational changes and functional properties of whey protein isolate-polyphenol complexes formed by non-covalent interaction. Food Chem. 364, 129622 https://doi.org/10.1016/j.foodchem.2021.129622.

Meng, Y., Hao, L., Tan, Y., Yang, Y., Liu, L., Li, C., Du, P., 2021. Noncovalent interaction of cyanidin-3-O-glucoside with whey protein isolate and β-lactoglobulin: focus on fluorescence quenching and antioxidant properties. LWT–Food Sci. Technol. 137, 110386 https://doi.org/10.1016/j.lwt.2020.110386.

Møller, A.H., Wijaya, W., Jahangiri, A., Madsen, B., Joernsgaard, B., Vaerbak, S., Hammershøj, M., der Meeren, P.V., Dalsgaard, T.K., 2020. Norbixin binding to whey protein isolate - alginate electrostatic complexes increases its solubility and stability. Food Hydrocolloids 101, 105559. https://doi.org/10.1016/j.foodhyd.2019.105559.

Nwachukwu, I.D., Udenigwe, C.C., Aluko, R.E., 2016. Lutein and zeaxanthin: production technology, bioavailability, mechanisms of action, visual function, and health claim status. Trends Food Sci. Technol. 49, 74–84. https://doi.org/10.1016/j.tifs.2015.12.005.

Qie, X., Chen, Y., Quan, W., Wang, Z., Zeng, M., Qin, F., Chen, J., He, Z., 2020. Analysis of β-lactoglobulin–epigallocatechin gallate interactions: the antioxidant capacity and effects of polyphenols under different heating conditions in polyphenolic–protein interactions. Food Funct. 11, 3867–3878. https://doi.org/10.1039/D0FO00627K.

Qiu, C., Zhao, M., Decker, E.A., McClements, D.J., 2015. Influence of protein type on oxidation and digestibility of fish oil-in-water emulsions: gliadin, caseinate, and whey protein. Food Chem. 175, 249–257. https://doi.org/10.1016/j.foodchem.2014.11.112.

Rasera, M.L., de Maria, A.L.A., Tavares, G.M., 2023. Co-aggregation between whey proteins and carotenoids from yellow mombin (Spondias mombin): impact of carotenoids' self-aggregation. Food Res. Int. 169, 112855 https://doi.org/10.1016/j.foodres.2023.112855.

Rawel, H.M., Rohn, S., Kruse, H.P., Kroll, J., 2002. Structural changes induced in bovine serum albumin by covalent attachment of chlorogenic acid. Food Chem. 78 (4), 443–455. https://doi.org/10.1016/S0308-8146(02)00155-3.

Ren, Y., Liu, T., Liu, H., Zhu, Y., Qi, X., Liu, X., Zhao, Y., Wu, Y., Zhang, N., Liu, M., 2022. Functional improvement of (−)-epicatechin gallate and piceatannol through combined binding to β-lactoglobulin: enhanced effect of heat treatment and nanoencapsulation. J. Funct.Foods 94, 105120. https://doi.org/10.1016/j.jff.2022.105120.

Steiner, B.M., McClements, D.J., Davidov-Pardo, G., 2018. Encapsulation systems for lutein: a review. Trends Food Sci. Technol. 82, 71–81. https://doi.org/10.1016/j.tifs.2018.10.003.

Uhrínová, S., Smith, M.H., Jameson, G.B., Uhrín, D., Sawyer, L., Barlow, P.N., 2000. Structural changes accompanying pH-induced dissociation of the β-lactoglobulin dimer. Biochemistry 39 (13), 3565–3574. https://doi.org/10.1021/bi992629o.

Wang, Y., Yang, C., Zhang, J., Zhang, L., 2023. Influence of rose anthocyanin extracts on physicochemical properties and in vitro digestibility of whey protein isolate sol/gel: based on different pHs and protein concentrations. Food Chem. 405, 134937 https://doi.org/10.1016/j.foodchem.2022.134937.

Xu, L., Echeverria-Jaramillo, E., Shin, W.S., 2022. Physicochemical properties of muffins prepared with lutein & zeaxanthin-enriched egg yolk powder. LWT–Food Sci. Technol. 156, 113017 https://doi.org/10.1016/j.lwt.2021.113017.

Yi, J., Fan, Y., Yokoyama, W., Zhang, Y., Zhao, L., 2016. Characterization of milk proteins–lutein complexes and the impact on lutein chemical stability. Food Chem. 200, 91–97. https://doi.org/10.1016/j.foodchem.2016.01.035.

Zahoor, I., Dar, A.H., Dash, K.K., Pandiselvam, R., Rusu, A.V., Trif, M., Singh, P., Jeevarathinam, G., 2023. Microwave assisted fluidized bed drying of bitter gourd: modelling and optimization of process conditions based on bioactive components. Food Chem. X 17, 100565. https://doi.org/10.1016/j.fochx.2023.100565.

Zhang, Y., Wright, E., Zhong, Q., 2013. Effects of pH on the molecular binding between β-lactoglobulin and bixin. J. Agric. Food Chem. 61 (4), 947–954. https://doi.org/10.1021/jf303844w.

Zhang, Y., Li, R., Xu, Z., Fan, H., Xu, X., Pan, S., Liu, F., 2024. Recent advances in the effects of food microstructure and matrix components on the bioaccessibility of carotenoids. Trends Food Sci. Technol. 143, 104301 https://doi.org/10.1016/j.tifs.2023.104301.

Zhao, C., Miao, Z., Yan, J., Liu, J., Chu, Z., Yin, H., Zheng, M., Liu, J., 2022. Ultrasound-induced red bean protein–lutein interactions and their effects on physicochemical properties, antioxidant activities and digestion behaviors of complexes. LWT–Food Sci. Technol. 160, 113322 https://doi.org/10.1016/j.lwt.2022.113322.

Zhu, J., Wang, C., Gao, J., Wu, H., Sun, Q., 2019. Aggregation of fucoxanthin and its effects on binding and delivery properties of whey proteins. J. Agric. Food Chem. 67, 10412–10422. https://doi.org/10.1021/acs.jafc.9b03046.

Zhu, J., Li, K., Wu, H., Li, W., Sun, Q., 2020. Multi-spectroscopic, conformational, and computational atomic-level insights into the interaction of β-lactoglobulin with apigenin at different pH levels. Food Hydrocolloids 105, 105810. https://doi.org/10.1016/j.foodhyd.2020.105810.